LIDAR MEASUREMENTS OF TEMPERATURE USING RAYLEIGH LIGHT SCATTERING IN THE LOWER STRATOSPHERE FOR THE PERIOD FROM MAY TO DECEMBER OF 1995

V.V. Zuev, V.N. Marichev, S.L. Bondarenko, S.I. Dolgii, and E.V. Sharabarin

Institute of Atmospheric Optics,
Siberian Branch of the Russian Academy of Sciences, Tomsk
Received March 25, 1995

In this paper we present some results of nighttime temperature measurements in May–December 1995. The data presented in the form of 29 profiles for the altitude interval 15–30 km. In the general case, vertical temperature distribution well agrees with the model one. At the same time, at altitudes 15–20 km we have revealed the tendency of temperature to increase in July and to decrease in November–December, as compared to the model behavior. The warming noticed in November at altitudes 25–30 km can be related to the process of fall reconstruction of the air mass circulation in the stratosphere. To check up the reliability of lidar data, we conducted two measurements of temperature with lidar and radiosonde. The discrepancy was within 5°C for the 15–25 km altitude range, i.e. within the measurement error.

Sandford was the first researcher who made an attempt of using the signals due to Rayleigh (molecular) scattering to reconstruct atmospheric density and temperature profiles.[1] He used a lidar with a ruby laser. But the ends were achieved by Hauchecorne and Chanin, who reported in 1988 about obtaining density and temperature profiles in the 35–75 km altitude range.[2] During last fifteen years, the lidar equipment has passed the stages of intense development and now Rayleigh lidars are widely used in many laboratories[3] and when working under some international programs, for example, in network aimed at detecting stratospheric changes (NDSC).

We started our temperature measurements from the signals due to Rayleigh light scattering at the Siberian Lidar Station (57°N, 85°E, Tomsk) in the fall of 1994. We have obtained the profiles of temperature in the upper stratosphere and mesosphere (35–75 km) using the lidar with a receiving mirror 2.2 m in diameter and a transmitter built around a Nd:YAG laser (second harmonic, wavelength of 532 nm).[4] Then temperature sounding was continued with the lidar having a receiving mirror 1 m in diameter and a transmitter built around a XeCl laser with SRS conversion in a cell filled with hydrogen (wavelength of 353 nm). In this case, our observations covered the lower stratosphere (10–40 km altitude range). Laser output power at 353 nm was 30–50 mJ, pulse repetition rate was 40–50 Hz, beam divergence was within 0.2 mrad, and the receiving system's field of view was 0.5 mrad. Echo-signals were recorded in the photon counting mode with the spatial resolution of 100 m and the total of 510 strobes per a channel. Time of lidar signal integration needed to

obtain one temperature profile at altitudes up to 40 km was 20–40 min.

Temperature profiles were reconstructed from the Rayleigh (molecular) light scattering signals based on the one-to-one correspondence between the molecular backscattering coefficient, $\beta_\pi(H)$, and the atmospheric density, $\rho(H)$, at the altitude H. If the law of ideal gas state and thermodynamic equilibrium hold and there are no aerosol layers within the interval sounded, the expression for temperature T has the following form:

$$T(H) = \frac{P^2(H)}{N(H)\,H^2} \times$$

$$\times \left[\frac{N(H_m)\,H_m^2}{P^2(H_m)}\,T(H_m) + \frac{1}{R^*} \int\limits_{H_m}^{H} \frac{N(h)\,h^2\,g(h)\,\mathrm{d}h}{P^2(h)} \right], \quad (1)$$

where

$$P^2(H) = \exp\left[-2 \int\limits_0^H \alpha(h)\,\mathrm{d}h \right]. \quad (2)$$

In Eqs. (1) and (2), R^* is the specific gas constant, g is acceleration of gravity, $N(H)$ is the lidar signal, $P(H)$ is the transmittance of molecular atmosphere from the level of lidar to the altitude H, α is the molecular scattering coefficient at 353 nm wavelength, H_m is the maximum height from which a sufficiently reliable signal can be recorded.

© 1996 Institute of Atmospheric Optics

Note that the above expression for temperature T differs from that derived in Ref. 2:

$$T(H) = \frac{g(H)\,\Delta H}{R^*\,\ln\,(1 + X)}\,, \qquad (3)$$

$$X = \frac{\rho(H)\,g(H)\,\Delta H}{Q\,(H + \Delta H/2)}\,, \qquad (4)$$

where Q is the pressure, and ΔH is the spatial resolution. This expression was derived in Ref. 2 from the conditions of pressure difference at upper and lower boundaries of a selected layer, while we derived our expression considering pressure as a mass of integral column of the atmospheric density. In addition, we took into account signal attenuation due to molecular scattering, whose contribution becomes significant when operating in the lower stratosphere and the upper troposphere. The comparison of results of temperature calculations by Eqs. (1) and (3) with regard for the molecular transmission P^2 showed quite good agreement.

Let us now consider the results of temperature sounding for May–December 1995. They are shown in Fig. 1 as 29 separate profiles. In the figure, along with the lidar temperature profiles (solid curves), set out are model profiles (dashed curves) for midlatitude summer, winter, and off-season. It should be noted that lidar profiles at the plots are given for altitudes 5 km below $H_{\max}$. It is due to the necessity to decrease the influence of error caused by somewhat arbitrary assignment of a model value $T(H_{\mathrm{m}})$ to the real temperature. One can see that vertical temperature distribution is generally in a good agreement with the model one. As expected, lidar temperature profiles have individual structure, because they were obtained at different nights. The profiles for May 11 and 12 coincide closely with the model ones. Then, beginning from May 17, some temperature drop is observed at altitudes from 15 to 20 km. This drop is seen in the plots on May 23 and June 9 and 12. From early July the lidar temperature profile (3.07.95) passes through the model one, then a temperature rise is observed in the lower part of the profiles on July 5 to 9. On July 10 and 11 temperature distribution comes to the model one again. In the succeeding period, our observations were interrupted until September 23. On this night the temperature distribution coinciding with the model one was observed. However, on September 26, its redistribution occurred at lower altitudes, and the temperature dropped by 10°C in 16–20 km altitude range and rose by 15°C at a 15 km altitude. In the next days from the late September to the early November, the profiles had practically identical structures, i.e., reduced temperature at lower altitudes

and temperature coincident with that given by the model at higher altitudes. In the middle of November (14.11.95), temperature distribution came close to the model one. In the next days, November 15, 21 and 22, temperature redistribution occurred to the above-mentioned profile with reduced temperature in the lower part and that elevated up to 16°C above 25 km level. Unstable temperature distribution was noticed on November 29 and December 3. By late December, strong cooling-out took place at altitudes below 20 km; at the same time on the profile for December 25 one can see warming with the maximum at a 25-km altitude and a 12°C deviation from the model one.

Note that the described dynamics of the vertical temperature distribution in the stratosphere is based on the results of lidar observations. For a complete analysis and interpretation of the dynamics of vertical temperature distribution, wider information is needed including synoptics for the altitude range under consideration, data of independent measurements, etc. We are planning to use synoptic maps and radiosondes data in our further investigations. However, already now the following facts can be stated. First, in the middle summer (July) stable warming of the atmosphere is observed in the 15–20 km altitude range and, on the contrary, in October–December cooling of the atmosphere takes place at the same altitudes. In May, June and September the vertical temperature distribution is close to the model one. The temperature rise noticed in November at altitudes of 25–30 km may be an indication of a seasonal process of the circulation change. Second, on many figures, as an altitude increases, the temperature oscillations about the model profile become more and more pronounced. In a number of cases, these oscillations exhibit a wavy structure. From the physical point of view, this circumstance may be explained by the fact of appearance, in the stratosphere, of internal gravity waves,[5] for which temperature plays the role of a tracer.

From the viewpoint of measurement data reliability, one should keep in mind that the measurement error also increases with the altitude. This may lead to the noticeable discrepancies in temperature. In order to evaluate the reliability of lidar data, we have performed test study. They consisted in simultaneous measurements of temperature profiles with a lidar and a radiosonde. Figure 2 shows the temperature profiles obtained with a lidar and a radiosonde in the 15–25 km altitude range at night of July 3 and 6, 1995. One can see from comparing the data that maximum discrepancy throughout the altitude range does not exceed 5°C. Taking into account errors in balloon and lidar measurements as well as their separation in time and space the results of calibration can be considered to be quite satisfactory, and thus the lidar data can be considered as sufficiently reliable.
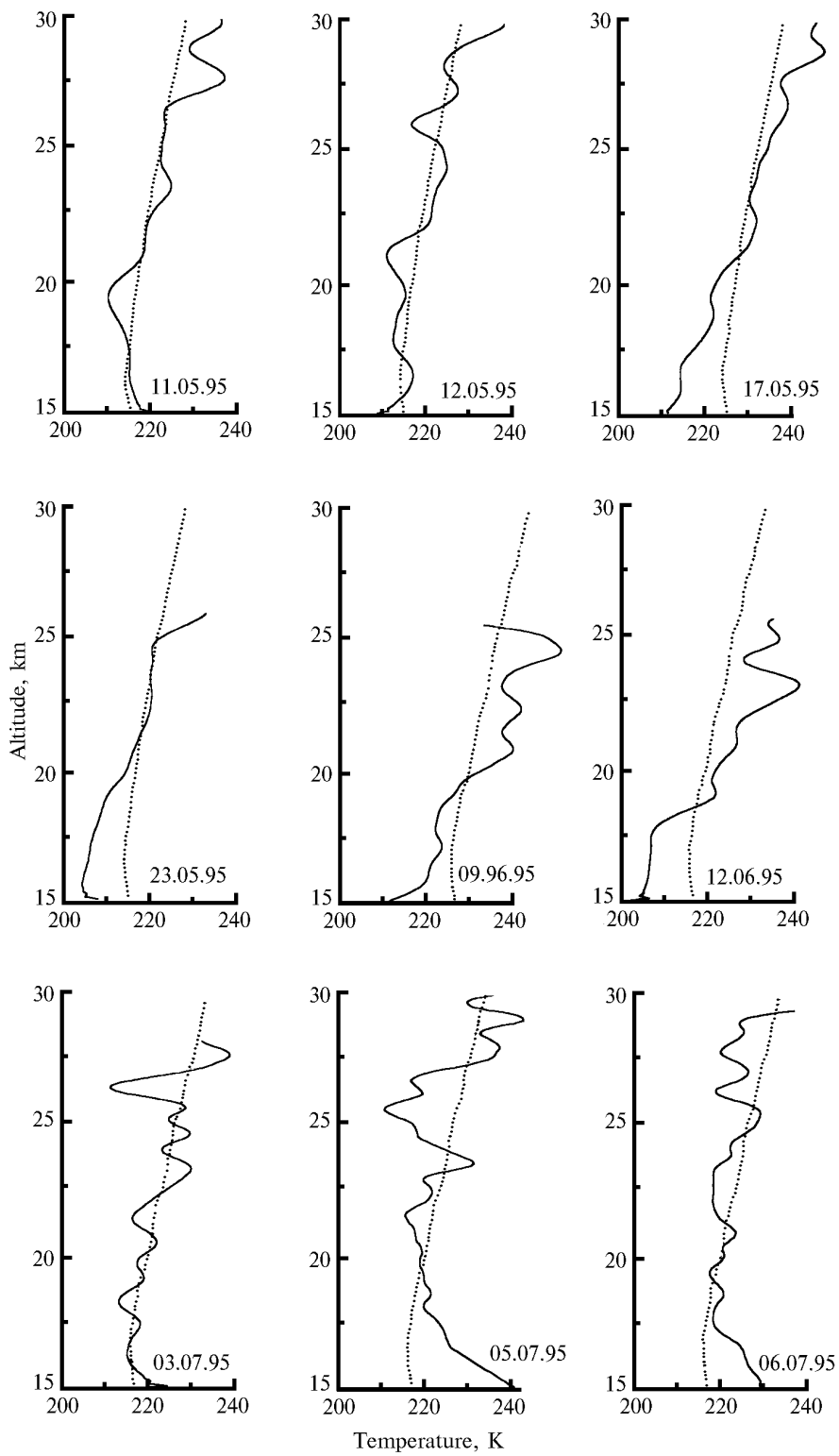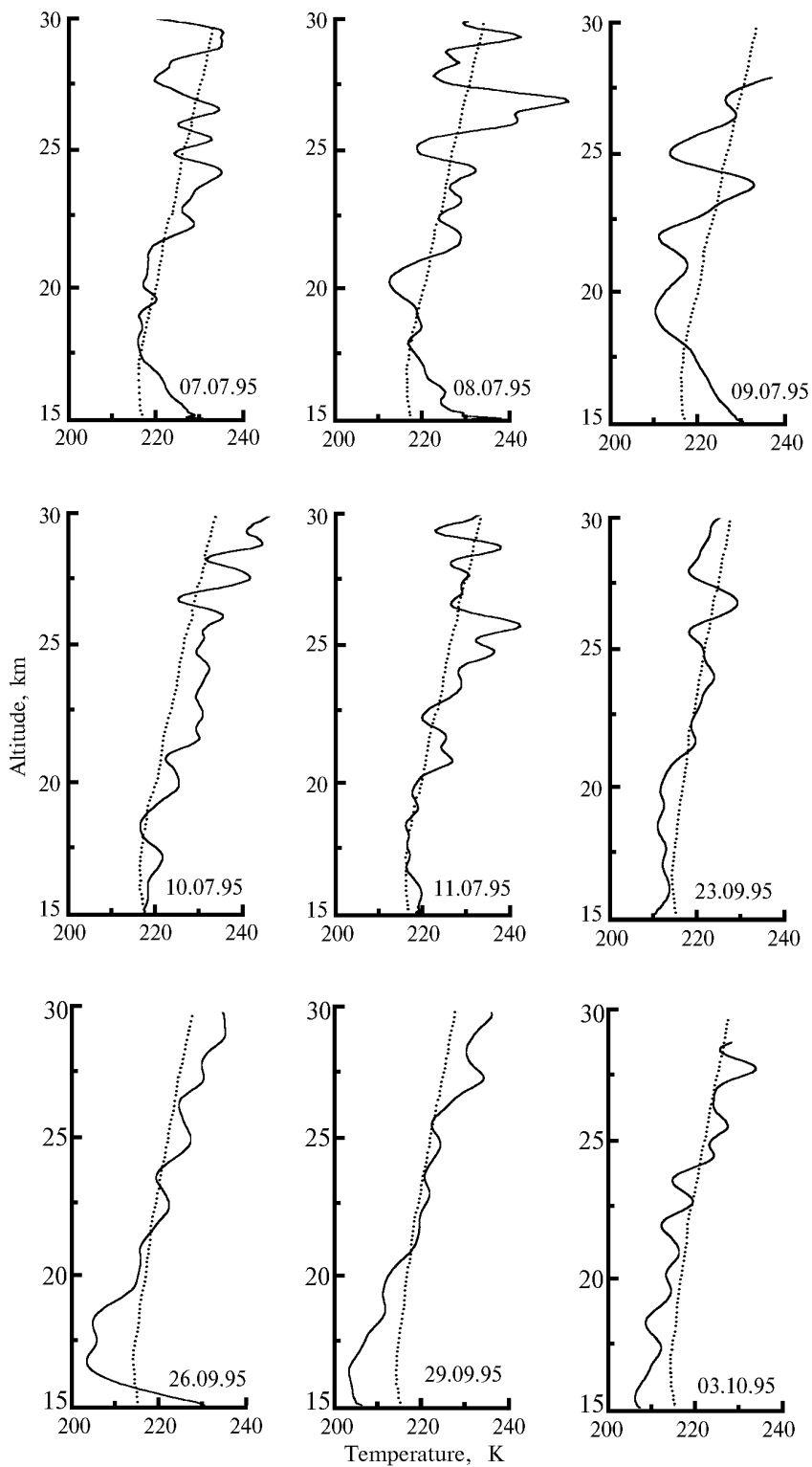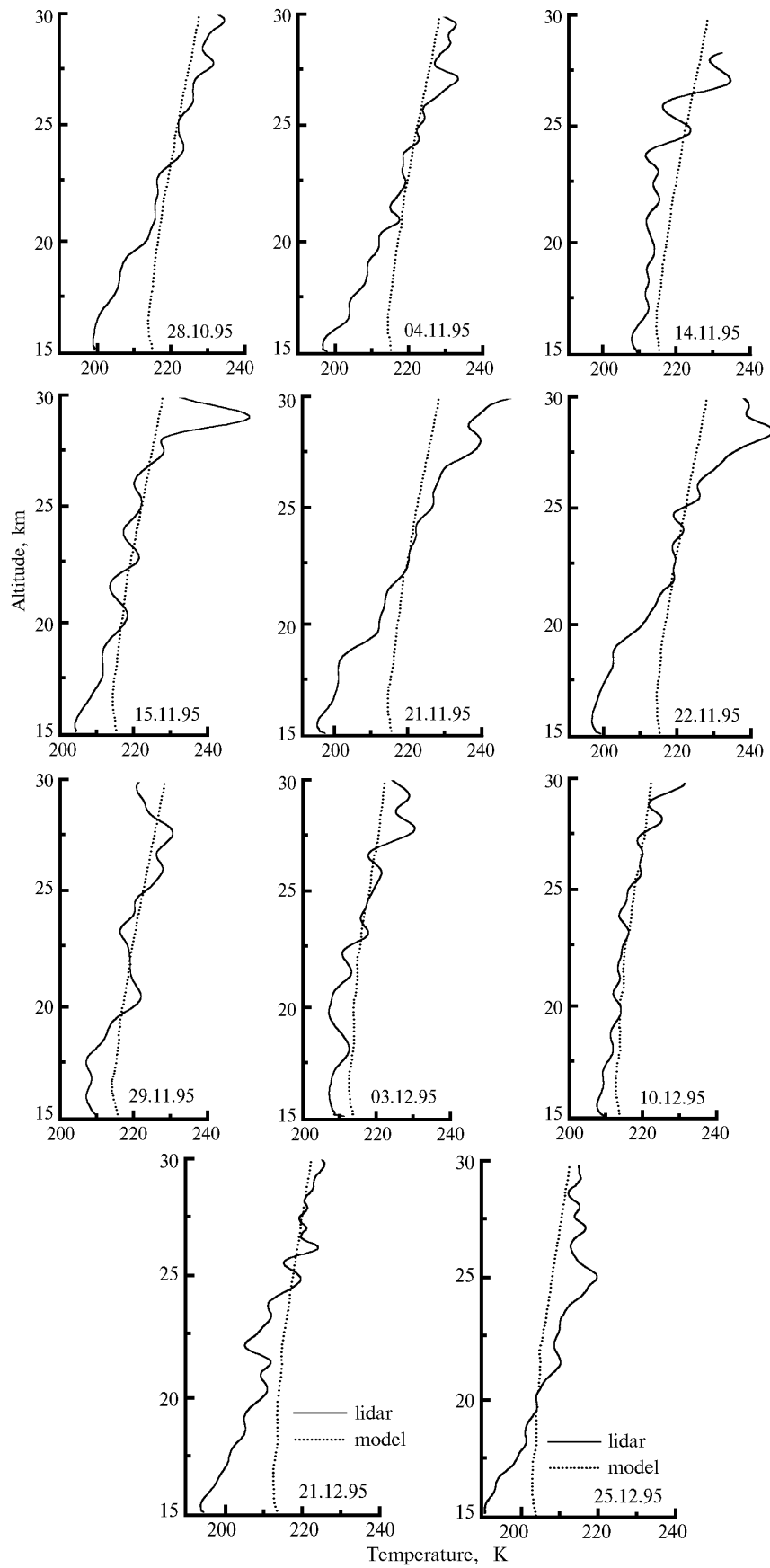
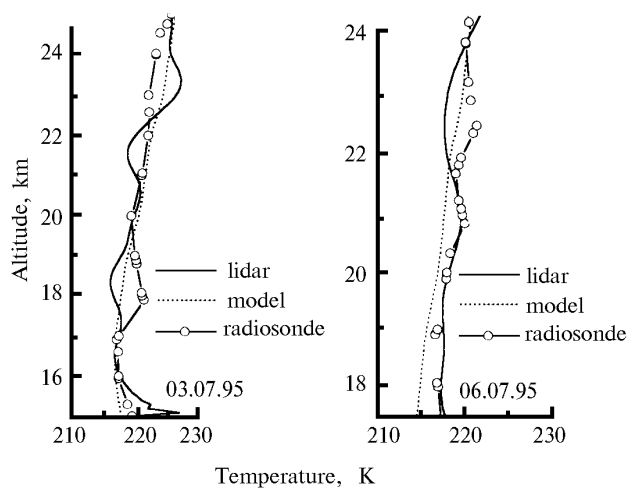FIG. 1. Dynamics of the vertical temperature distribution.

FIG. 2. Intercomparison of temperature profiles obtained with a lidar and a radiosonde.

REFERENCES

1. M.C.W. Sandford, J. Atmos. Terr. Phys., No. 29, 1657–1662 (1967).
2. A. Hauchecorne and M.-L. Chanin, Geophys. Res. Lett. **7**, No. 8, 565–568 (1980).
3. *3-rd Inter. Lidar Researchers Directory,* compiled by M.P. McCormick, NASA Langley Research Center, Hampton, Virginia, Feb. 1993,
4. S.L. Bondarenko, V.D. Burlakov, M.I. Grishaev, V.V. Zuev, V.N. Marichev, and V.L. Pravdin, Atmos. Oceanic Opt. **7**, Nos. 11–12, 899–900 (1994).
5. C.R. Philbrick, SPIE **1492** Earth and Atmospheric Remote Sensing, 76–83 (1991).